

DOE/PC/88948--T2

**DEPARTMENT OF MECHANICAL ENGINEERING
COLLEGE OF ENGINEERING
MICHIGAN STATE UNIVERSITY**

DOE/TC/88948--T2

DE92 014031

226

23 February 1992

Dr. Shelby Rogers
Project Manager
Mail Stop 922-L
U.S. Department of Energy
P. O. Box 10940
Pittsburgh, PA 15236

Study of Flow Properties of Wet
Solids Using Laser Induced Photo Chemical
Anemometry. April-June 1991.

Dear Dr. Rogers:

Quarterly Technical Progress Report April-June 1991

Contract DE-AC22-88PC88948

OVERVIEW

MAY 10 1992

During this period we have made:

- **Progress in the Analysis of the Accuracy of the Technique**
- **Progress in Firming the Foundations of LIPA for Solid-Liquid Mixtures**
- **Progress in the Construction of better prototype skimmers**

To get a 'feel' for the difference in solid liquid content that developed in the core vs the annulus of the pipe. Obtained qualitative flow visualization of the thicker core/more liquid annulus flow.

- **Continued progress in chemically manufacturing both more red Europium imbedded CaF₂ and green liquid Flowlite.**

As discussed previously, this is the material of choice for use in our experiments for the solid phase that is photoluminescent. We also continued to make more green Flowlite for the liquid phase. However during this period it became apparent that without the requested centrifuge, we could not make enough of this material to fill the vertical pipe flow device, and thus we would have to use silica gel for our runs.;

- **Progress in understanding the coupling of LIPA chemicals and dynamic range and timing**

1) During this period we attempted to do our two color imaging of the mixture at high solids loading. In the course of setup we had a failure of our ITT image intensified camera. Diagnosing the intermittent problem required a large part of the available time. After sending it to both the primary and secondary supplier of the components, it was determined that the image tube was the culprit. All data taken up to that point was no good. But more importantly, this piece of equipment was a) paid for but funds from other sources but available for use on the contract. and

MASTER

aka

MAR 18 1992

b) we did not have funds available in the contract to pay for repair or replacement. However, the college cost shared in a camera that could do the job, and we helped to determine the best product, hoping to use it for our project. This was a KODAK Ektapro 1000 which was purchased for summer delivery.

Presented results in an invited paper at the ASME symposium for two phase flow in Portlan Oregon June 24-26 1991.

DETAILS

Progress in the Analysis of the Accuracy of the Technique

LIPA is a non-intrusive measurement technique, which, in principle, requires only a clock and a ruler for calibration. Thus, it potentially can provide high accuracy results for flows over the entire range of speeds discussed above. An error analysis follows which indicates the expected error resulting from double differencing a grid to obtain vorticity.

Consider one mesh from the grid as shown in Figure 3-2. If the mesh width is ϵ and the maximum line displacement between the reference and data images is $1/2$ of the mesh width, then after a time Δt the mesh will distort to the primed position. The spanwise vorticity component is defined:

$$\omega_z = \partial v / \partial x - \partial u / \partial y$$

$$= \left[\frac{(y_1' - y_1'') / \Delta t - (y_2' - y_2'') / \Delta t}{(x_2' - x_2'')} \right] - \left[\frac{(x_1' - x_1'') / \Delta t - (x_4' - x_4'') / \Delta t}{(y_4' - y_4'')} \right]$$

where,

$y_1' - y_1'' = \Delta y_I = 1/2\epsilon$	$x_1' - x_1'' = \Delta x_I = 1/2\epsilon$
$y_2' - y_2'' = \Delta y_{II} = 1/2\epsilon$	$x_4' - x_4'' = \Delta x_{II} = 1/2\epsilon$
$y_4' - y_1'' = \Delta y_{III} = \epsilon$	$x_2' - x_1'' = \Delta x_{III} = \epsilon$
$t_2 - t_1 = \Delta t$	

the uncertainty in the measurement of vorticity ($\delta\omega_z$) is thus,

$$(\delta\omega_z)^2 = (\partial\omega_z / \partial\Delta y_I \cdot \delta\Delta y_I)^2 + (\partial\omega_z / \partial\Delta y_{II} \cdot \delta\Delta y_{II})^2$$

$$+ (\partial\omega_z / \partial\Delta y_{III} \cdot \delta\Delta y_{III})^2 + (\partial\omega_z / \partial\Delta x_I \cdot \delta\Delta x_I)^2$$

$$+ (\partial\omega_z / \partial\Delta x_{II} \cdot \delta\Delta x_{II})^2 + (\partial\omega_z / \partial\Delta x_{III} \cdot \delta\Delta x_{III})^2$$

$$+ (\partial\omega_z / \partial\Delta t \cdot \delta\Delta t)^2$$

Estimates of the magnitudes of the terms are:

$$\begin{aligned} \partial\omega_z / \partial\Delta t &= -((1/2\epsilon - 1/2\epsilon) / \epsilon) / (\Delta t)^2 \cong 0 \\ \partial\omega_z / \partial\Delta y_I &\cong 1 / \Delta t \cdot \epsilon \\ \partial\omega_z / \partial\Delta y_{II} &\cong 1 / \Delta t \cdot \epsilon \\ \partial\omega_z / \partial\Delta y_{III} &\cong (1/2\epsilon - 1/2\epsilon) / \Delta t \cdot \epsilon^2 \cong 0 \\ \partial\omega_z / \partial\Delta x_I &\cong -1 / \Delta t \cdot \epsilon \\ \partial\omega_z / \partial\Delta x_{II} &\cong 1 / \Delta t \cdot \epsilon \\ \partial\omega_z / \partial\Delta x_{III} &\cong -(1/2\epsilon - 1/2\epsilon) / \Delta t \cdot \epsilon^2 \cong 0 \end{aligned}$$

Therefore,

$$\begin{aligned} (\delta\omega_z)^2 &= (\delta\epsilon / 2\epsilon\Delta t)^2 + (\delta\epsilon / 2\epsilon\Delta t)^2 \\ &\quad + (\delta\epsilon / 2\epsilon\Delta t)^2 + (\delta\epsilon / 2\epsilon\Delta t)^2 \\ &= 4(\delta\epsilon / 2\epsilon\Delta t)^2 \end{aligned}$$

Finally,

$\delta\omega_z = (1 / \Delta t)(\delta\epsilon / \epsilon)$
--

to the first order in ϵ . For example (see Figure 3-2) assume that the mesh spacing is 1000 μm , the line width is 100 μm , and that the image is digitized and analyzed in such a way that we have a 10% reading error associated with locating the center of the 100 μm line, i.e. $\delta\epsilon = 10 \mu\text{m}$, so $\delta\epsilon/\epsilon = 0.01$. If Δt , the time between two frames is 0.01 sec, $\delta\omega_z = (1 / \Delta t)(\delta\epsilon / \epsilon) = 1/\text{sec}$.

The technique has been calibrated in an unsteady Stokes' layer flow by Falco and Chu (1987), for which the exact solution of the Navier-Stokes equations is known. These results show that strain-rate and vorticity can be measured to an accuracy of $\pm 1 \text{ sec}^{-1}$, which is consistent with the above analysis.

DISCLAIMER

This report was prepared as an account of work sponsored by an agency of the United States Government. Neither the United States Government nor any agency thereof, nor any of their employees, makes any warranty, express or implied, or assumes any legal liability or responsibility for the accuracy, completeness, or usefulness of any information, apparatus, product, or process disclosed, or represents that its use would not infringe privately owned rights. Reference herein to any specific commercial product, process, or service by trade name, trademark, manufacturer, or otherwise does not necessarily constitute or imply its endorsement, recommendation, or favoring by the United States Government or any agency thereof. The views and opinions of authors expressed herein do not necessarily state or reflect those of the United States Government or any agency thereof.

Although it may appear at first thought that the spatial resolution of LIPA is going to be less than that of particle imaging techniques, which can use very small particles, this is not necessarily the case. An important practical consideration is that the spatial resolution to which the location of the center of a single line can be found is not strongly coupled to the thickness of the laser lines or to the thickness of the ensuing photoluminescent lines (which are initially somewhat thinner). Because the marker is non-intrusive, a marked spot can be quite large compared to the point of measurement interest, as long as the center of the spot can be accurately determined from the image by image processing techniques. Although relatively thick lines may be used in LIPA, the motion of the field will not be constrained by the presence of the lines (irrespective of how large they are). This is, in general, not the case when a particle is used as a marker of the fluid, because the finite size of the marker distorts the flow it is in. During the time interval between marking and recording, the action of diffusion on the excited fluid lines is symmetric, simply spreading them about their centers. However, if the thickness of the lines is large enough that macroscopic flow field variations occur across them, the position of the centers will reflect an average that is biased towards the high velocity regions when imaged after the time delay. Thus, the laser line thickness and the time delay need to be optimized for the flow problem. As a result of these considerations, variations in the thickness of the laser lines across the measurement volume do not need to be considered separately. This lack of sensitivity to the thickness of the laser lines is important for solid-liquid flows because small index of refraction variations will focus and defocus the laser lines causing variations in their thickness along their length. Furthermore, the resolution of a vorticity measurement depends upon the mesh size of the grid, which can be adjusted independently of the grid line thickness. Finally, the field over which the measurements are made is also independent of these constraints, and depends only upon the number of grid lines created (here the key constraint is often the output energy of the laser).

When the lines are recorded on either film or video tape, the limiting resolution is dependent solely on the ratio of pixel size (or film grain) to the smallest length scales that need to be resolved in the flow. If the pixel size is small compared to the flow scales then the formation of relatively thick lines, on the order of $100\ \mu\text{m}$, imaged across ten pixels, results in greater accuracy than imaging thinner

lines, on the order of 20 μm , across 2 pixels, when sub-pixel averaging is used to determine the centers. Furthermore, more advanced noise reduction techniques can be used on thicker grid lines without fear of breaking the individual lines into discontinuous segments. This is in contrast to PIV or holography where $\sim 10 \mu\text{m}$ particles must be clearly defined in space, requiring enough pixels over these dimensions so that the particles are obviously separable from the noise in the image. Then enough particles must be averaged to allow correlation techniques to be implemented, which decreases the resolution to the order of a millimeter (if there are scales smaller than a millimeter, their contribution may not be evenly weighted by the particles imaged in that area). Thus, these considerations relax two important aspects of an experimental design for LIPA, the laser line width and the resolution of the imaging system.

Coupling of LIPA chemicals and dynamic range and timing

In our search for appropriate chemicals, the tie-in with timing is essential. One of the drawbacks of fluid or particle tracking techniques is that they can present limitations on dynamic range in flow situations where strong velocity gradients are present. In a quasi-uniform flow there is, of course, no problem because the time between frames can be chosen to obtain optimum displacement of the grid lines. If strong gradients are present, LIPA can avoid most of the limitations on dynamic range through a simple tactic. When used with a chemical that works in Excite-Self-Decay, or Sensitize-Delay-Excite modes, where the shuttering is done by the imaging system by using an imaging rate that will be appropriate for the highest velocities to be encountered in the field of view, the dynamic range is extended to be as wide as needed. To measure the slower velocities, the investigator simply skips an appropriate number of frames to allow the lower velocity regions to move the marked fluid over a distance predetermined to give the desired measurement accuracy. If the Excite-Forced-Decay mode is being used, the laser that forces the excited state to decay must have a repetition rate high enough to accomplish the task.

Figure 3-7 indicates an example of a typical timing sequence for experiments in the Excite-Self-Decay mode. In this sequence the high speed camera sends a signal every four revolutions to the

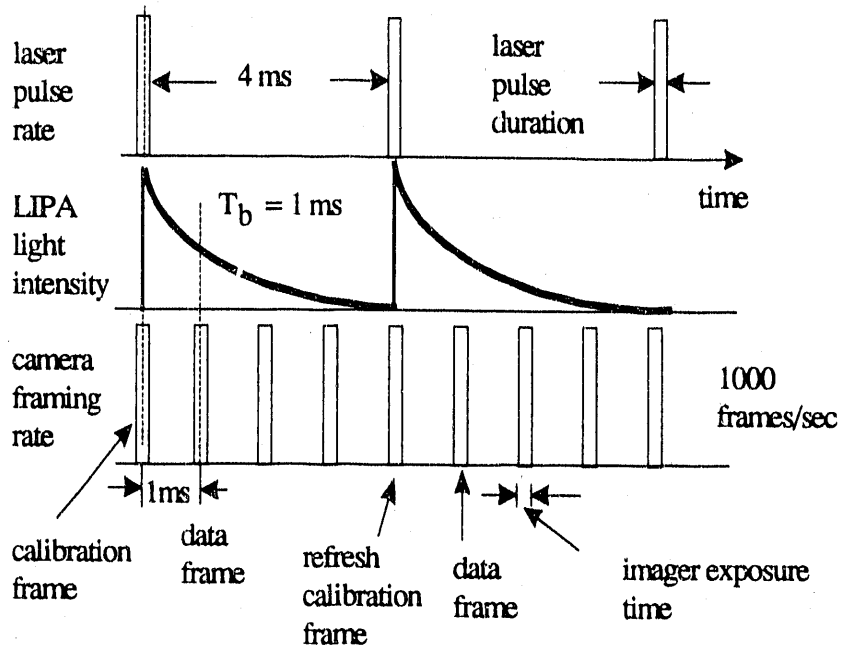


FIGURE 3-7. A typical timing sequence for experiments of the Excite-Forced-Decay mode in which a high speed imager is used to record the results.

laser, which pulses in nanoseconds, exciting the chemical in the fluid. Here, a chemical with a 1 ms lifetime is shown, which is suitable for a 1000 frame/sec imager (film camera or solid state), and a 250 Hz laser. In this timing arrangement, the first frame is the calibration (containing the laser energy), and the subsequent three frames contain data, with the highest quality data frame being the one after the laser is triggered. The overall decay of the chemical is indicated to be four framing intervals. The optimum framing rate is governed by the flow, as is the lifetime of the chemical chosen. If a high shear region exists, the dynamic range can be extended by simply increasing the framing rate, to have frames close enough to account for larger displacements per unit time in the high velocity regions.

Progress in Firming the Foundations of LIPA for Solid-Liquid Mixtures

LIPA can be extended to investigate the flow dynamics in the interior of refractive index matched solid-liquid flows. The extension is based upon two ideas. The first is that by index matching the doped two-phase mixtures, light can pass through the mixtures in straight lines, enabling essentially the same technique to be applied. The second idea is to dope the phases of the mixtures with

photoluminescent chemicals that radiate different colors. Color can be used to distinguish between the solid and liquid phases. It can even be used to distinguish particles of different size distributions from the liquid they are in.

We will discuss the use of LIPA to measure the average flow properties of a solid-liquid mixture, and to separately but simultaneously measure the dynamics of the liquid and the solid phases. We then extend the discussion to procedures for three-dimensional measurements of the above cases.

Although LIPA can be used for three-dimensional measurements in single phase flows, these techniques are described in this section because of the particular value of such measurements in solid-liquid flows. Next, techniques which enable simultaneous flow visualization and LIPA are discussed. This is followed by an outline of the measurement of wall shear stress using LIPA. LIPA imaging issues are then considered. In all of the above scenarios, once the flow is index matched and doped with photoluminescent chemicals, qualitative flow visualization of the mixture as a whole, or of either phase can be made, by putting a sheet of laser light into the flow, instead of a grid of laser lines.

3.3.1. Refractive Index Matching

The use of LIPA in solid-liquid flows requires refractive index matching. This constraint is also essential to the use of LDA or particle imaging techniques for measurements in solid-liquid flows. Majumdar et al. (1987a, b) in their work on stereo particle imaging discuss the precision with which index matching must be done for large particles. Nouri et al. (1987) have discussed the constraints put on LDA measurements, and have, so far, been able to make measurements in flows with concentrations up to 14% by volume. With careful matching it appears possible to use LDA at higher concentrations (Abbas and Crowe (1989) worked with concentrations to 30%). However, LIPA is inherently less sensitive to the consequences of index of refraction mismatch than LDA. Three important index matching issues are: the error incurred by variability in the degree to which beams coming through different regions of a flowing mixture cross to form intersections of the grid, the accuracy in locating a beam crossing position when there is variation, and the effect of refractive

index induced beam width variations. In the following, we explore the crucial matter of the consequences of index of refraction variations in some detail.

We first note that LIPA does not require that the beams cross perfectly, or even with the same degree of error from instant to instant. Figure 3-9 shows a perfect beam crossing (I), and examples of possible alignment mismatches (II-V) that may occur from instant to instant in a somewhat imperfectly matched solid-liquid flow. The errors that these misalignments cause for LIPA are entirely due to the difference of the location from the hypothetical position of the grid plane. The index of refraction differences that caused the displacements of the laser lines do not affect the subsequent motion of the photoexcited lines by the fluid. As long as there are no scales in the flow of the order of the misalignment distance, there will be no additional relative displacement of the two lines about the intersection region. This error in the location of the grid intersections normal to the hypothetical grid plane is defined by the difference of the center of area of the locus of the circumferences of the intersecting laser lines, and thus is at a location outside of the hypothetical grid plane which is, at maximum, one half of a beam width -- if the beams have any common intersection. Since the photoluminescent molecules at the laser beam intersections receive more incident energy, they typically photoluminesce more brightly (as much as doubling the brightness), or undergo a stronger color change, so that a missed crossing can be detected in any data field. Thus, if desired, we could use the intensity of photoemission to detect whether beams have crossed in the third dimension, and establish a discriminator level, below which the data is not used. However, in general, even at a location where the beams do not cross (see Figure 3-9 IV, for example), in all but the most severe circumstances they will be close enough relative to the smallest scales in the flow (which would be the order of the grid's mesh size by design -- typically 10 times the line width), that we will obtain valid data, with the aforementioned decrease in spatial resolution in the third dimension. If the distortion were the order of the grid mesh size, this would be observed in the grid plane as well. Thus, in severe situations, the in-plane information could also serve as the basis of a criterion for rejecting a data point (or data set).

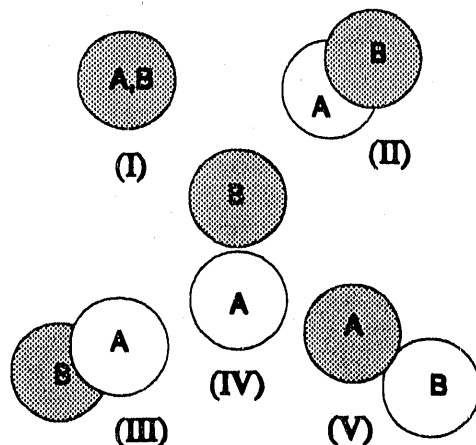


FIGURE 3-9. *Cross-sectional views of two crossing laser beams (drawn as circles) of the LIPA grid. (I) represents a perfect crossing, while (II-V) represent a range of probable changes in the crossings with time due to unavoidable refractive index variations that may exist in the flow.*

In general, there is no loss of resolution in the plane of the imager because the projections, although distorted by the (ever present, small) index mismatch, will appear to the imager to cross. Since it is only the difference in the positions of the crossing, over the allowed time interval, that is used to obtain LIPA data, in the plane of the imager there is no apparent problem. Thus, in the two-component data obtained from a three-dimensional flow field using the LIPA technique, the index of refraction variations show up only in the fact that the data is actually at a slightly different coordinate position in the third dimension. If we are ensembling the results of many realizations, then position errors similar to those created in the third direction become errors in positions of the intersections of the various members of the ensemble in the grid plane, because the laser lines are refreshed and sent into the fluid for each member of the ensemble, and the index of refraction fluctuations may cause differences between realizations. Of course, the index of refraction differences between realizations (which are typically only small fractions of a second apart) may be less than any differences within a given realization.

Since running a typical solid-liquid flow loop test requires significant time, it is difficult to keep the temperature constant over the course of a test, and one would expect small fluctuations in index of refraction from instant to instant. However, as we have suggested, LIPA can be used to make very useful measurements under these circumstances. It is important to note that LDA would result in loss of information, or bad information, for all options in Figure 3-9 except the perfect crossing. And,

even if the beams do cross sufficiently well to get a good signal, one does not have information on the position change of any of the measurement volume coordinates, as is naturally available by using the LIPA technique. Furthermore, these variations will likely be accompanied by variations in the angles of beam crossing, and positions of the two beam waists, which are important to know in the LDA technique. Changes in the angle of beam intersection are not important in the LIPA technique because, once again, only the relative positions between time intervals matter. Comparative experiments to determine the relative insensitivity to index of refraction variations of LIPA with other techniques, particularly LDA, have not yet been performed.

An issue that is of particular importance for LIPA in index matched solid-liquid flows is that only one wavelength of light can be matched exactly, but at least two are needed for LIPA; the excitation laser wavelength, which is typically in the ultraviolet (see Table 3-1), and the visible emission from the chemicals. We propose the following procedure to reduce the distortions. Index match the solid-liquid mixture to optimize the transmission of the incident laser beam wavelength. This results in the best quality excitation. Immediately after excitation, the chemicals used will emit visible light, which will not be perfectly index matched on its passage out of the mixture to the imager. Since the index mismatch will result in the light appearing to be at slightly different position than the laser beam, the first image should be made immediately after the laser pulse. We should use this, rather than the laser lines as the reference grid. Then the grid is imaged again after the flow has moved it an appreciable amount. The displacements are calculated between these two images, and the results can be referred back to the geometric location of the crossing laser lines. Since the grid displacements are only a fraction of a grid mesh, the additional changes in the index mismatch due to grid motion by the flow will, in general, result in negligible additional error. Obviously, the development of chemicals that can be excited closer to the visible spectrum, or even within it, would reduce or eliminate the need for this procedure.

3.3.2. Data Acquisition

3.3.2.1. Average Flow Properties of Either Phase, or of the Mixture

To measure the average flow properties of the mixture, it is not necessary to distinguish between the liquid and solid phases. The procedures for the use of LIPA are thus identical to procedures in single phase LIPA discussed above, except that an index matched mixture must be created, which has an appropriate chemical doped into the liquid or into the solid phase or into both phases. Appropriate chemicals that enable us to index match the phases after doping are discussed below. Although both phases can be doped with the same chemical to obtain average flow properties, it may be convenient to dope each phase with different chemicals to enable a mixture to be used for other experiments in which the capability of distinguishing them is needed (see below). For the present purposes, one would simply not distinguish the phases either with the imaging system or during the data analysis. Under this doping arrangement, if it is desirable to measure the flow properties of either the liquid or of the solid, this can then be done by the simple addition of a filter that transmits either the wavelength of the chemical doped in the liquid or the solid, in front of the camera. A schematic of the optical arrangement is shown in Figure 3-10 (in this drawing and the following ones flat-sided index matched pipe enclosures, which would be helpful to reduce near-wall distortions of received light, are not shown). We will use the schematic convention of portraying the film size by the camera size. Typically, object-to-image magnification would be in the range of 5:1 to 0.5:1.

3.3.2.2. Simultaneous Measurement of Both Solid and Liquid Phases

To enable separation of the dynamics of the solid and the liquid phases, or even a further separation of the dynamics of different size distributions of particles, the constituents to be distinguished need to be doped with chemicals that radiate different colors when excited. The correct choice of chemicals can enable excitation with the same laser radiation. Thus, only one grid need be impressed into the mixture. A discussion of the chemicals for doping is deferred to the next section. Here we shall

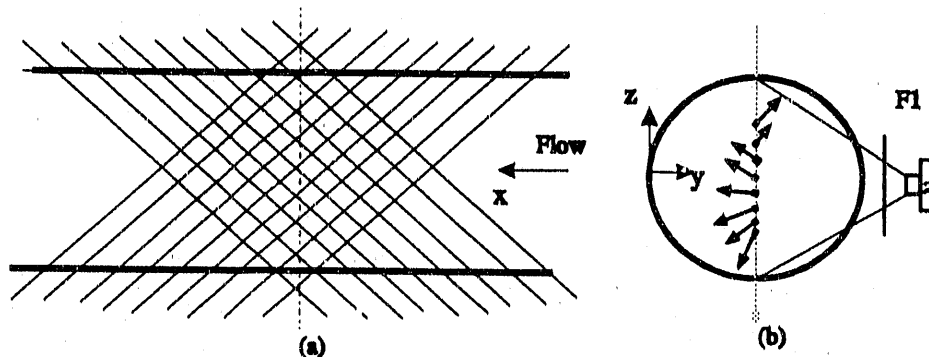


FIGURE 3-10. LIPA arrangement to obtain average flow property measurements of a solid-liquid mixture or flow property measurements of each component separately. a) Axial slice (x coordinate direction) in the plane of the initial laser induced grid of lines, b) slice perpendicular to the pipe axis (y-z plane), showing possible out of plane motion that may occur, and the field of view of the camera. For measurement of the combined properties, both phases are marked and left indistinguishable in the analysis. With the addition of a filter (F1), the investigator could choose to measure only the response of the solid or the liquid phase. The shaded line is the end view of the laser grid. (In this drawing and the following ones flat-sided pipe enclosures, used to assist in index matching the pipe wall material so as to reduce near-wall distortions of received light, are not shown).

assume, for ease of discussion, that the solid phase has been doped to radiate red and the liquid phase has been doped to radiate green.

Figure 3-11 shows an image acquisition arrangement that can give simultaneous solid and liquid phase dynamics. It consists of using a split field view for synchronization, to lower potential distortion (especially if film is used), and for economy. The color filters in front of each mirror, M1, will transmit light coming only from the solid or only from the liquid phase. Thus, on one half of each data frame we get the data for the liquid phase, and on the other half we get the data for the solid phase. Although we are using only one camera (either black and white film or electronic imaging -- or color film or color electronic imaging can be used), the optical setup is identical to an arrangement of two cameras (which are indicated by the dotted outlines at the positions where the apparent cameras would be). These cameras are both looking at the flow at a slightly different angle. (The angle is exaggerated in Figure 3-11). Thus the depth of field of the lens must accommodate the sine of the half angle of the image separation of the in-grid-plane field of view (for example, 5 degrees will result in a depth of field of 0.087 times the field of view). Furthermore, the components

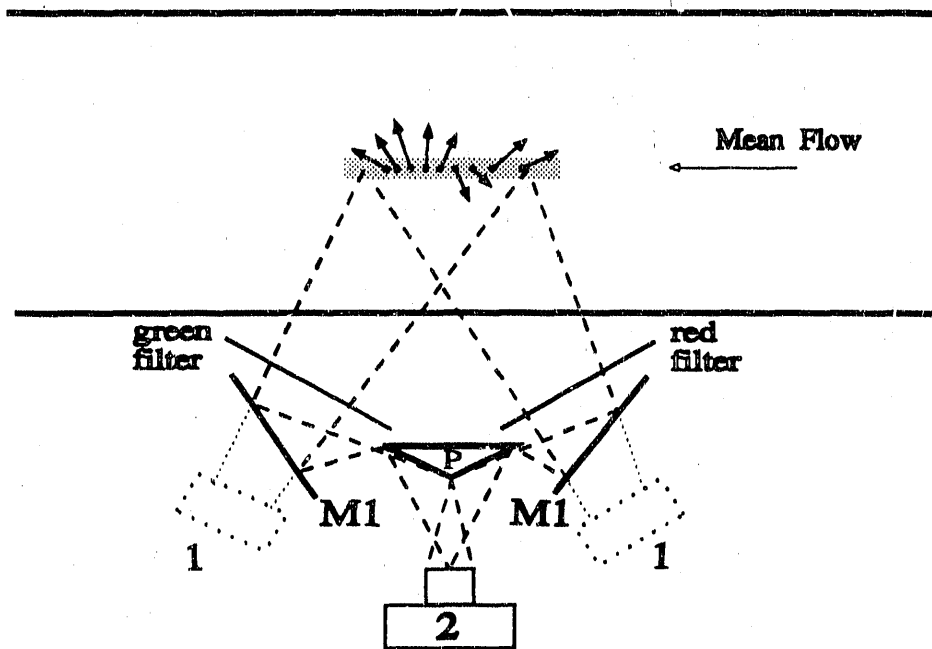


FIGURE 3-11. Plan view of a data acquisition arrangement to enable simultaneous measurement of both liquid and solid phases; the grid is formed perpendicular to the page in the plane containing the shaded line, and would look like that in Figure 3-10 from the side. The mirrors eliminate the need for two imagers (indicated by dotted lines (1)). Arrows indicate distortions of the grid normal to its plane of formation, which determine the imaging system's depth of field. The shaded region width indicates the needed depth of field, but the arrows are drawn longer to make the effect clear to the reader. If an arrow is green (color emitted by the fluid, say), then its emitted light will pass through the green filter, left side mirror (M1) to the face silvered prism (P) and to the right portion of the real imager (2). The light emitted from the particles, which if red, will pass through the red filter and the left portion of the imager, will record the velocity of particles (which may be anywhere along the grid lines). Dashed lines indicate the field of view of the imaging system, the overlap of which provides simultaneous data

of the velocity recorded will be slightly different for the particles and the fluid using this arrangement. The differences can be kept small by reducing the angle between the pseudo imagers to a minimum. From the point of view of flow dynamics, this arrangement is preferable to that shown in Figure 3-12 (which corresponds to rotating the assembly 90 degrees), because the differences in the relative accuracy of the left and right imaging are in the direction of the flow in which there are either no average differences or, at worst, slow changes (moving dunes for example). The above orientation also keeps the imaging optics and camera differences constant in the direction of mean shear, thus allowing the greatest accuracy.

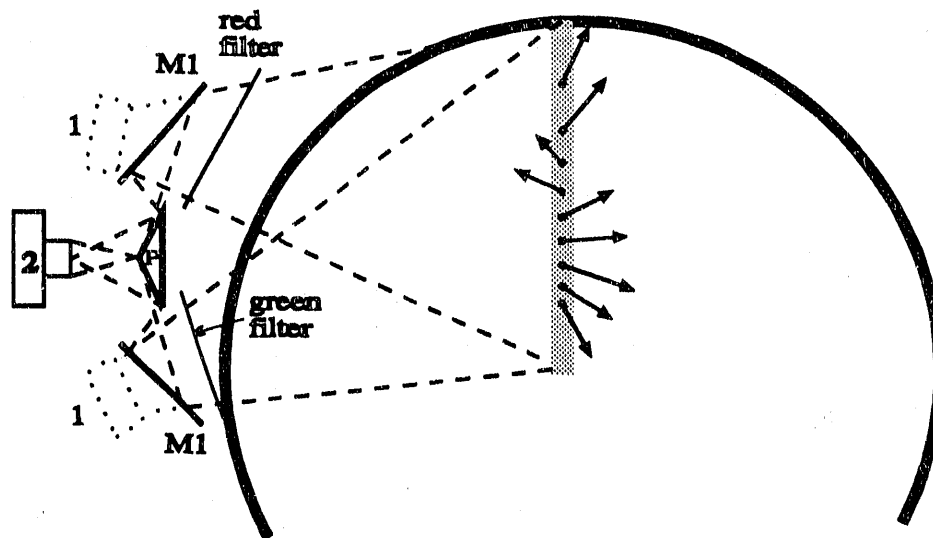


FIGURE 3-12. Use of the above configuration to measure axial and radial components of the fluid and the particle velocity fields. This arrangement puts the left and right imaging differences in the same direction as the mean shear, increasing measurement error, but has the advantage of requiring minimal optical access. Nomenclature is the same as for previous figure.

The view of Figure 3-12 is one in which the flow is coming out of the page, and we are looking end-on at the grid (so we don't see the mesh). This configuration has the advantage of needing only a small ultraviolet transmitting access window for laser light access, and a disc (if a pipe flow is being investigated) of glass or plexiglass for recording the images, and thus it allows measurements to be more easily made in existing metal flow systems.

Another configuration, shown in Figure 3-13, can be used to eliminate the differences inherent in any left-right sided arrangement. It still only requires one imager. The view here is again one in which the flow is coming out of the page, and again we are looking end on at the grid (so we don't see the mesh). The left side mirror/filter arrangement will get the same view of fluid velocities as the right side mirror/filter arrangement gets of the solid particles, since the depth of field is exactly the same. This relaxes the constraints on the lens, enabling faster lenses to be used. The investigator would set the depth of field to include the maximum expected excursion of the fluid or particles from the initial plane of the grid lines (these excursions are indicated by the arrows). In this arrangement, both left and right side images have exactly the same precision at any position across the pipe, so a larger field

of view is possible. Essentially the same visual access is required as for the configuration of Figure 3-12.

Of course two imagers can be used in an arrangement where they are on opposite sides of a pipe, for example. Figure 3-14 illustrates one possibility. The use of two imagers doubles the imaging resolution (the full imaging resolution can be used for each phase), and has the additional benefit of enabling the chosen delay time to be different for each imager. In a flow regime where a moving bed existed, it might be of interest to have a longer delay time for the solid phase measurements, since the solid would be moving at a different average speed than the liquid. The disadvantage is largely in the costs of the additional imager and associated synchronization electronics.

In general the use of filters as described above overcomes the need for carefully distinguishing different colors on a single piece of color film or on a color video camera. Because the phosphorescent chemicals used in LIPA emit at well defined frequencies, they can be sharply bandpass filtered. Without the filters, the excited lines would appear to have a brownish-orange color in general, because there is a mixture of both fluid and solid particles along each line and at the intersections of the grid, and thus a mixture of the two colors red and green, (using our color scheme). It is possible to filter after imaging, but the non-linear distortions of the imagers reduce the accuracy of this approach. Furthermore, filtering at acquisition time enables the use of black and white film, image intensifiers or image converter cameras, which don't distinguish color.

We note a few additional points. First, if the highest accuracy is required near the wall, the optical axis of the imaging optics should be located near the wall. For this purpose the symmetrical arrangements indicated in the above figures would be rearranged (in the sense that Figure 3-12 has been). Second, each planned limitation of the size of the field of view will enable higher resolution within the more limited field of view. Third, a simpler system, in which there is no spatial overlap of fluid and particulate information, i.e., the fluid velocities measured in the left half of the pipe and the particle velocities measured in the right half of the pipe, could simply use color filters to split the field and record particle and fluid velocities on different halves of the imager, without the use of the above optical systems. This arrangement could be used to obtain long time averaged statistics for

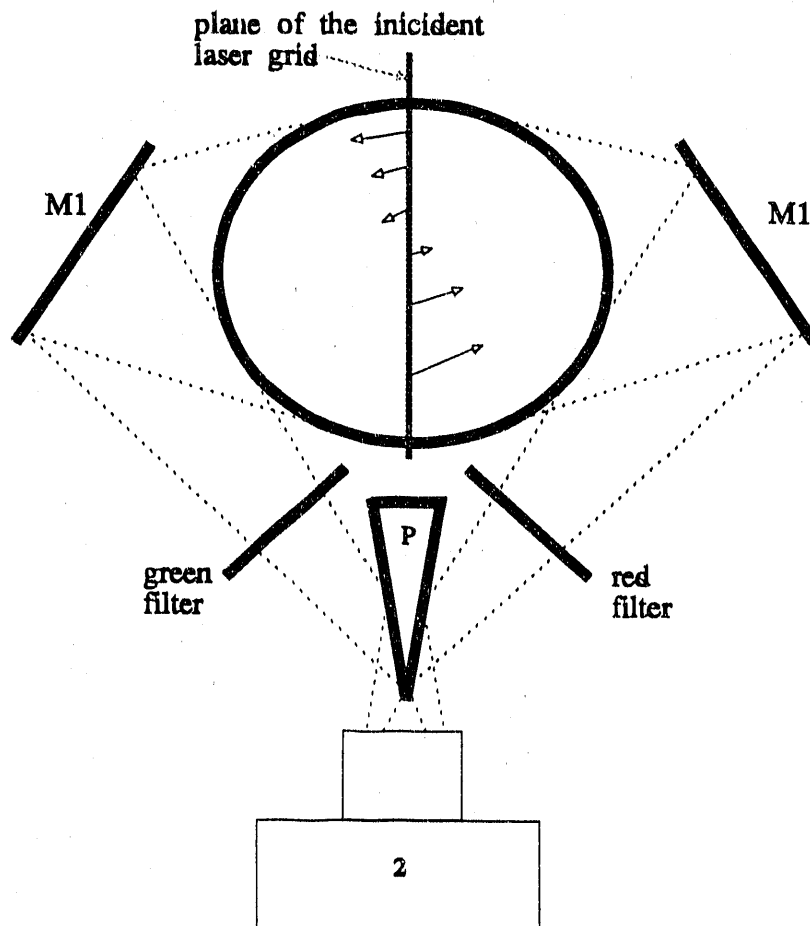


FIGURE 3-13. Another data acquisition arrangement to enable simultaneous particle and fluid velocities using LIPA. Here the optical paths for both the fluid and the solid are the same, enabling a wider field of view without 'left/right' imaging biases. The apparatus identification numbers are the same as above.

each phase. Fourth, it should be emphasized that if the resolution chosen is sufficient to record the motion of individual particles, then particle velocity information will be available all along the paths of the excitation laser radiation, not only at the grid intersections. Finally, as indicated above, the use of color to separate phases, can be extended to include the separation of particles from different size distributions, as well as separation of the phases. If more than two colors are to be separated out using filters, it may be advisable to use multiple imagers.

Ensemble averaging the data obtained by these methods at each intersection point over a large number of images will result in the velocity, vorticity and stress fields of the particles of the liquid. Correlating data from two grid intersections of either marked liquid or marked solid particles can yield pair distribution functions. Because we are making multi-point measurements, we can also

obtain three-point correlations, and other higher order statistics of the information of the components in the grid plane.

3.2.6. Advantages of LIPA Measurements

The advantages of LIPA are summarized below. One aspect of the LIPA technique that should be singled out is the exact way in which it incorporates the effects of three-dimensionality of a flow field. When a single grid and a single imaging system with its imaging plane parallel to the initial grid plane is employed, we obtain the projections of the three-dimensional distortions of the initially planar grid onto the plane of the imager. This only requires that the distortion in the third dimension remain within the depth of field of the imaging system. Thus, LIPA does not have the inherent difficulty of laser sheet confined particle tracking techniques, such as PIV, where either the first or second image of a particle may not be recorded because its trajectory carries it through the boundaries of a light sheet due to three-dimensional motions.

In summary, the advantages of the LIPA technique are:

- Instantaneous measurements of velocity, velocity gradients, Reynolds stresses, vorticity and strain-rate made over an area,
- Direct wall shear stress measurements,
- Interpretation of all results is simple and direct,
- Simple calibration depends only on a clock and a ruler,
- Simple data acquisition,
- Not limited by interferometric quality access,
- Data reduction can be automated,
- Data storage is minimal,
- Can be set up to give highly accurate space-and-time-resolved measurements over a large range of velocities,
- Non-intrusive, and particles are not necessary,
- Can be used in Newtonian or non-Newtonian gases, liquids or solid/liquid mixtures,
- Three-dimensional measurements of the velocity field, the complete stress tensor and vorticity vector over an area are possible (as we describe below),
- Standard wavelengths of ultra-violet and blue lasers can be used to excite many chemicals with long lifetimes,
- Quantitative measurements can be combined with flow visualization of the doped chemicals,

- Mixing can be studied by using more than one chemical,
- Potentially can be combined with LIF (Laser Induced Fluorescence) to give concentration information along with the kinematic data.

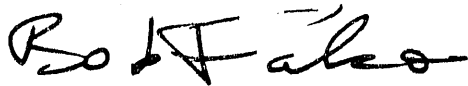
The chief disadvantages of LIPA are:

- Specific chemicals must be found for flow velocities and fluids of interest,
- Cost of the chemicals,
- Need for ultraviolet light to excite many chemicals.

We will see that these attributes of LIPA form a foundation that can be enhanced to result in a technique that can enable systematic studies of solid-liquid two-phase flows as outlined above.

Overall progress has been made firming the underpinnings of the use of the LIPA technique for use as a two-phase flow diagnostic, and all indications are that it will be able to provide badly needed new data about these flows.

Sincerely,



Bob Falco
PI

END

**DATE
FILMED**

7 / 2 / 92

